

Thermophysical properties of pure HF0-1132a and HF0-1132a & HFC-134a binary blends' refrigerants from 240 K to 300 K using MD simulation

Sanzida Akter

Department of Mathematics, Jagannath University

Rifat Ara Rouf

Department of Physical Sciences, Independent University

Md. Rakibul Hasan

Department of Mathematics, Dhaka University of Engineering & Technology

Md. Sarwar Alam

Department of Mathematics, Jagannath University

<https://hdl.handle.net/2324/7395491>

出版情報 : Proceedings of International Exchange and Innovation Conference on Engineering & Sciences (IEICES). 11, pp.8-15, 2025-10-30. International Exchange and Innovation Conference on Engineering & Sciences

バージョン :

権利関係 : Creative Commons Attribution-NonCommercial-NoDerivatives 4.0 International



Thermophysical properties of pure HFO-1132a and HFO-1132a & HFC-134a binary blends' refrigerants from 240 K to 300 K using MD simulation

Sanzida Akter¹, Rifat Ara Rouf², Md. Rakibul Hasan³ and Md. Sarwar Alam^{1*}

¹Department of Mathematics, Jagannath University, Dhaka-1100, Bangladesh

²Department of Physical Sciences, Independent University, Bangladesh

³Department of Mathematics, Dhaka University of Engineering & Technology, Dhaka-1100, Bangladesh

Corresponding author email: sarwardu75@gmail.com

Abstract: *The HFO-1132a refrigerant and its blends are considered for new generation refrigerants due to their zero ozone depletion potential and ultra-low global warming potential which can be used for various existing applications of HFC-134a with minor modification. The saturated vapor pressures of pure HFO-1132a and its three binary blends (HFO-1132a) + (HFC-134a) under various mole ratios are computed in the temperature range of 240 K-300 K using COMPASS II force field via molecular dynamics simulations in this paper. The saturated vapor-liquid densities of the pure HFO-1132a and its binary blends are also estimated. Moreover, the phase diagram with critical points of pure HFO-1132a and the three blends are also predicted. The results indicate that as the proportion of HFC-134a is increased in the blend, the saturated pressure decreases and the liquid density increases. In case of vapor density, it does not follow any consistent trend.*

Keywords: vapor pressure; saturated densities; phase diagram; HFO-1132a; MD simulation

1. INTRODUCTION

Heating, ventilation, air conditioning and refrigeration (HVAC&R) is one of the largest global industries, which is growing fast because of urbanization and rapidly advancing technologies. Even if CFCs and HCFCs are well known for their magnificent thermal performance, the Montreal Protocol of the European Union phases them out because of their high Ozone depletion potential (ODP). As the third generation refrigerants, HFCs are introduced, but their Global Warming Potential (GWP) is still alarming for the environment [1-2]. Recently, Hydrofluoroolefins (HFOs) become popular among the researchers because of their low GWP and ODP and are considered as fourth-generation refrigerants.

The HFO refrigerant HFO-1132a (1,1-Difluoroethylene) has achieved substantial adoption in refrigeration and air-conditioning sectors due to its environmental compatibility and favorable thermophysical performance attributes [3]. HFO-1132a holds great potential as a sustainable replacement for HFCs, because this refrigerant demonstrates an ultra-low GWP of 0.6 with zero ODP. The HVAC&R industry can be utilizing HFO-1132a in multiple residential and commercial applications under specified safety protocols because it processes A2L (mildly flammable) and low toxicity classification. However, study of the flammability, ensuring compatibility with HVAC&R materials of HFO-1132a and securing regulatory approval, is still ongoing. The analysis of HFO-1132a has turned towards investigating its molecular dynamics and thermodynamic properties in the refrigeration system. Several studies demonstrate that HFO-1132a maintains stable operation under diverse conditions, thus establishing itself as a promising choice for low-GWP refrigerant applications [4-7].

The researchers had studied the properties of HFO-1132a in multiple refrigeration and cooling system applications in early 1990s. Perera et al. [4] estimated

PvT properties and thermodynamic property correlations for refrigerant HFO-1132a. The obtained results deliver important information necessary to create efficient and sustainable low-temperature refrigeration systems. The International Institute of Refrigeration (IIR) performs assessments of HFO-1132[E] through its exploration of refrigerant blends under varied operational environments. The saturation pressures for the novel refrigerant R1132(E) is measured by Perera et al. [5]. Fedele et al. [8] worked on thermophysical properties of low GWP Refrigerants. The saturated pressure and vapor-phase pvT measurements of R1132a is obtained experimentally by Tomassetti and Nicola [9].

While specific research on HFO-1132a blends are limited, studies on other HFO-HFC blend have demonstrated promising results, suggesting that HFO-1132a+HFC-134a blends have great potential. Moreover, blends of HFOs with other refrigerants are practically chosen to produce working fluids with lower flammability and higher volumetric refrigerant capacities compared to those of pure HFOs [10]. The HFC refrigerant HFC-134a provides excellent thermodynamic properties, so manufacturers use it extensively in both automotive air-conditioning systems and domestic refrigeration applications. However, HFC-134a demonstrates a high GWP value of 1430 that triggers substantial environmental problems even though the refrigeration industry must comply with climate change regulations. In 2023, the U.S. Environmental Protection Agency (EPA) implemented significant regulatory changes under the American Innovation and Manufacturing (AIM) Act to phase down the use of hydrofluorocarbons (HFCs), including HFC-134a, due to their high global warming potential (GWP). This law includes that servicing the existing infrastructures using HFC-134a will still be permitted. Lee et. al [11] investigated on the performance of the azeotropic mixture of HFO-1234yf and HFC-134a for HFC-134a applications.

Molecular dynamics (MD) simulation has been extensively used for computation of various thermophysical properties in the field of HVAC&R. Recently MD simulation has gained significant attention for being widely used in validating the experimental data; particularly in the field of refrigerants and their mixtures [12]. For example, the thermophysical properties of R1234yf, R1234ze(E), ternary blend R445a were assessed by Raabe [10,13] which showed good agreement with the experimental data. In 2014, Smith et al. [14] predicted the thermophysical properties and phase transition phenomena of R134a, R143a using MD simulation which is well aligned with the results of REFPROP. The saturation pressure and vapor-liquid equilibrium for binary blends of HFO-1234yf and HFO-1123 [15], the thermal properties of R448 and R449 [16], critical properties of HFO-1123 and its binary blends with R32, R134 [17] are obtained by Alam and Jeong using MD simulation. Hasan et al. [18] studied the condensation process of R600/R290 mixtures using MD simulation. In conclusion, MD simulation can effectively predict refrigerants thermodynamical properties like REFPROP and experiments.

The thermodynamic properties of binary blends HFO-1132a with HFC-134a for a variety range of temperatures is not available in open literature yet. Therefore, the saturation pressures of new low-GWP refrigerant blends HFO-1132a + HFC-134a under various compositions are calculated in the temperature range of 240 K to 300 K using molecular dynamics simulations. The saturated densities and critical points of HFO-1132a + HFC-134a blends with various compositions were computed from the MD simulation results. In addition, the saturated vapor pressures and critical points of pure HFO-1132a are also calculated for the same temperature range for comprehensive comparison with previously published data.

2. SIMULATION METHODOLOGY

In this research, MD simulations were performed using the COMPASS II [19] force field to examine the thermophysical properties of HFO-1132a alongside three blends of it with HFC-134a with the aid of Materials Studio program [20].

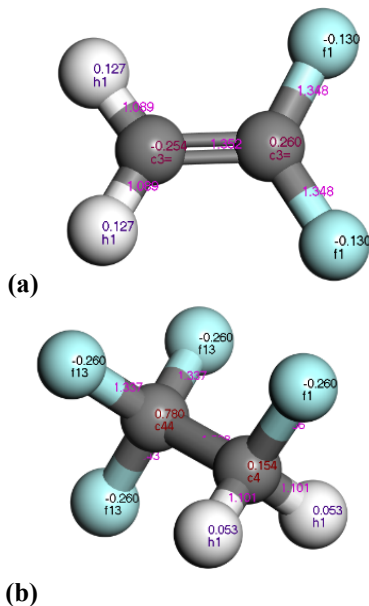


Fig. 1. Molecular structures of (a) HFO-1132a($\text{CH}_2=\text{CF}_2$); (b) HFC-134a(CH_2FCHF_3). The colour of C, H, and F atoms are grey, white and blue respectively.

Three-dimensional representation of HFO-1132a and HFC-134a were constructed as seen in Fig.1 and then geometry optimization dynamics were applied for optimizing the molecules geometrically. The parameters for C, H, and F atoms were fitted according to the COMPASS II force field. The COMPASS II force field employs ab initio and empirical parameterization elements which create compatibility throughout gaseous and condensed phases.

$$U = \sum_{LJ} \varepsilon_{ij} \left[2 \left(\frac{\sigma_{ij}}{r_{ij}} \right)^9 - 3 \left(\frac{\sigma_{ij}}{r_{ij}} \right)^6 \right] + \sum_{\text{elec}} \frac{q_i q_j}{r_{ij}} + \sum_{\text{bonds}} k_b (b - b_0)^2 + \sum_{\text{angles}} k_\theta (\theta - \theta_0)^2 + \sum_{\text{dihedral}} k_\phi (1 - \cos n\phi), n \geq 0$$

The simulations used cubic periodic boundary conditions to construct cells containing pure HFO-1132a and three binary blend compositions. The blend components received precise definitions through mole ratio and molecular mass percentage settings to achieve proper composition as shown in Table 1.

Table 1. Composition of components in the blend of HFO-1132a and HFC-134a

Blend s	Refrigerants	Mole ratio	Number of Molecules	Molecular mass (%)
Blend ¹	HFO 1132a	0.827	234	75
	HFC 134a	0.173	49	25
Blend ²	HFO 1132a	0.614	175	50
	HFC 134a	0.386	110	50
Blend ³	HFO 1132a	0.347	99	25
	HFC 134a	0.653	186	75

A study of up to 290 molecules was performed simultaneously in simulation cells that had numbers between 270 and 290. Figure 2 represents the primary configuration of 286 HFO-1132a molecule at density 0.135 g.cm^{-3} . A modified Lennard-Jones (LJ-9-6) potential modeled the van der Waals interactions along with Coulombic function-based electrostatic interactions measured through partial atomic charges. MD simulations are operated under NVT ensembles to explore the saturated vapor pressure for the temperatures 240 K to 300K. The simulation ran for 10 ns period and each computational step set to 1 fs. During equilibration, the system temperature was managed with Berendsen thermostats [21] for 2.5 ns and then 7.5 ns of production run simulation in NHL thermostat [22-24] where the decay constant sets at 1.0 ps.

To predict saturated densities of pure HFO-1132a and its three binary mixtures with HFC -134a, five simulation cells were constructed separately for each of these compounds at 270 K, 285K, 290K, 293K, and

298K. Then, equilibration simulation was run for 2.5 ns for each cell under MD-NPT simulation followed by a production run simulation during the next 5 ns at these temperatures for vapor densities. The time step was 1fs. The NHL thermostat and Barendsen barostat [25], with corresponding effective relaxation time, were applied to maintain the temperature and pressure of these cells.

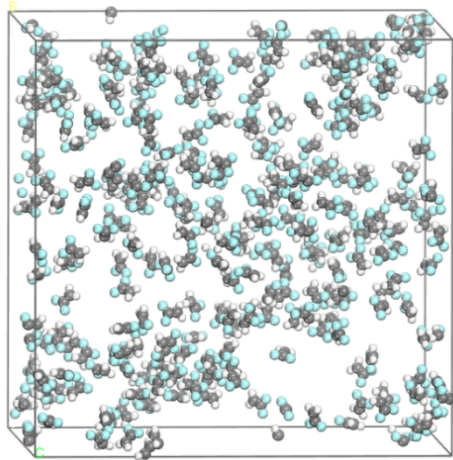


Fig. 2. Primary configuration of 286 of HFO-1132a molecule at density 0.135 g.cm^{-3}

The Materials Studio EQUILIBRIA module computed vapor-liquid coexistence curves together with critical temperatures and densities. The Gibbs Ensemble Monte Carlo method served to identify critical points with reference to measured saturated vapor-liquid phase-density data using MD simulations. The scaling law combined with the law of rectilinear diameters produced accurate predictions. This methodology produces exhaustive data about HFO-1132a phase behavior and thermophysical traits, which enable future experimental lab work and practical use.

3. RESULTS AND DISCUSSION

The saturated vapor pressure, saturated vapor-liquid densities and the critical values of temperature and density, the vapor-liquid co-existence curve of pure HFO-1132a and its three binary mixtures with HFC-134a were investigated in the present work. BIOVIA Material studio program was used to run molecular dynamics simulation with the aid of the COMPASS II force field.

3.1 Saturation pressure

Table 2 shows the simulation results for saturated vapor pressure of pure HFO-1132a and the blend¹⁻³. Simulation results of pure HFO-1132a were compared against experimentally measured data of Perera et al. [4] for temperatures from 240 K to 300 K. A good agreement between present MD simulated data and the experimental data of Perera et al. [4] is observed with 2.9 % of maximum error in Fig.3. Figure 4 represents saturation pressures of pure HFO-1132a and blend¹⁻³ as tabulated in Table 2. The results show excellent consistency. The present MD simulation model sustained reliable predictions for the results estimated for vapor pressures for HFO-1132a. These calculated values show promise for determining thermodynamic properties of refrigerant blends. The COMPASS II force field parameters with regard to both the intramolecular terms together with LJ parameters from this model are fully transferable for mixture components. These force

field potentials were utilized in previous MD simulation studies of Alam and Jeong [15-17] to predict results successfully. Figure 4 shows that the saturation pressures of HFO-1132a increased with temperature.

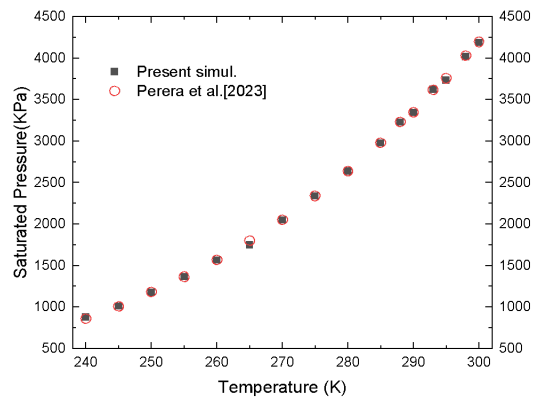


Fig. 3. Estimated vapor pressures of pure HFO-1132a from MD simulation and experimental data/

The COMPASS II force field model was extensively used to run MD simulations of three binary blends¹⁻³ of HFO-1132a and HFC-134a with various compositions of molecule mass and mole fractions. Figure 4 reveals that vapor pressure decreased steadily between pure samples of HFO-1132a and HFC-134a (REFPROP) together with their three binary blends. The vapor pressure dropped when HFC-134a molecule mass percentage increased and pure HFO-1132a decreased in the mixtures. Vapor pressure showed a substantial reduction at temperatures higher than 285 K as the HFC-134a molecular mass fraction shifted from pure HFO-1132a to blend¹ which contained 25% HFC-134a. HFC-134a composition growth failed to produce a significant reduction in vapor pressure after first composition increase stages. Observation on HFO-1132a and blend compositions 1 through 3 indicated HFC-134a strongly affected the vapor pressure behavior of each mixture.

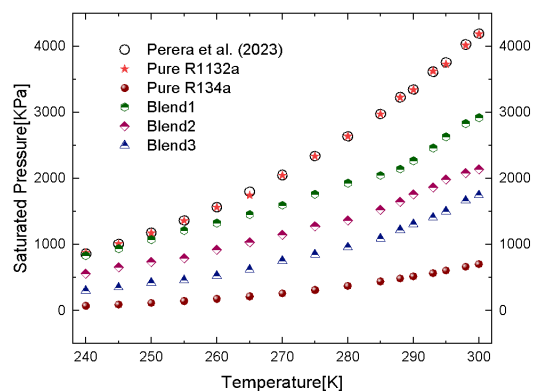


Fig. 4 Predicted saturated pressure of pure HFO-1132a, its three blends¹⁻³ with HFC-134a from current MD simulation and HFC-134a from REFPROP.

3.2 Density profile

The estimation of saturated vapor and liquid densities from MD simulation at five different temperatures of 270 K, 285 K, 290 K, 293 K, 298 K of pure HFO-1132a and its mixtures¹⁻³ with HFC-134a are demonstrated in Figure 5. Figure 5 shows that the vapor density of pure

HFO-1132a is notably higher than pure HFC-134a. On

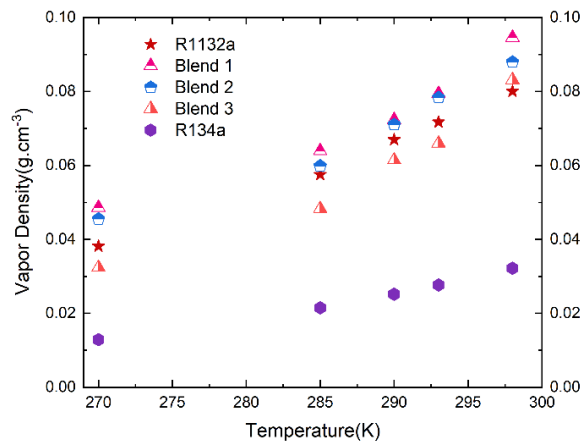
the other hand, the liquid density of pure HFO-1132a is significantly less than pure HFC-134a.

Table 2. Computed saturated vapor pressure of pure HFO-1132a, its three blends¹⁻³ with HFC-134a and REFPROP data of HFC-134a.

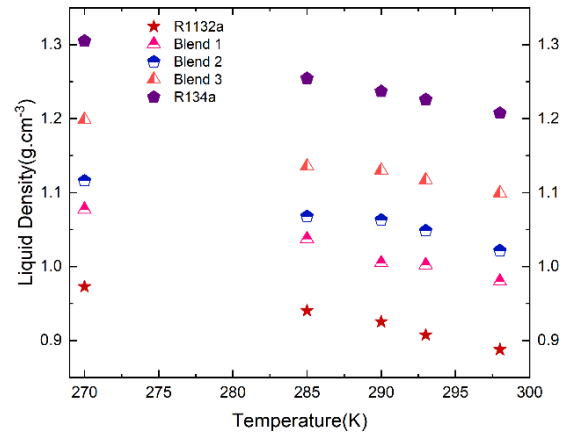
Temperature [K]	Pressure [KPa]						
	HFO-1132a (MD simul.)	Perera et al.[4]	Relative Error (%)	Blend ¹	Blend ²	Blend ³	HFC-134a (REFPROP)
240	878.0000	859.940	2.10014	834.0000	560.0000	304.0000	72.481
245	1010.484	1008.29	0.21759	939.0000	659.0000	354.0000	92.057
250	1174.776	1178.85	0.34559	1073.736	734.0000	423.0000	115.61
255	1364.381	1363.78	0.04406	1210.239	791.0000	463.0000	143.68
260	1564.744	1567.78	0.19365	1325.990	924.0000	525.0000	176.84
265	1747.637	1799.97	2.90743	1454.499	1037.312	626.0000	215.67
270	2047.011	2051.77	0.23194	1594.455	1144.469	725.0000	260.82
275	2337.906	2338.85	0.04036	1763.067	1274.540	848.0000	312.94
280	2637.430	2638.93	0.05684	1927.414	1363.219	959.0000	372.71
285	2974.507	2977.57	0.10286	2045.585	1528.168	1089.608	440.83
288	3226.986	3228.00	0.03141	2142.796	1650.158	1219.429	486.03
290	3341.532	3344.95	0.10218	2265.083	1760.965	1310.305	518.05
293	3623.745	3616.00	0.21418	2462.601	1863.603	1410.413	569.06
295	3731.965	3755.86	0.63620	2627.305	1985.478	1500.403	605.12
298	4015.850	4028.00	0.30163	2830.162	2078.130	1666.569	662.41
300	4186.360	4194.61	0.19668	2918.457	2141.253	1748.583	702.82

Table 3. Computed critical points of HFO-1132a, blends¹⁻³ and HFC-134a from GEMC simulation in comparison with experimental data [4], REFPROP [26] data.

Critical para.	HFO-1132a		Blend ¹	Blend ²	Blend ³	HFC-134a	
	GEMC	Perera et al.[4]	GEMC	GEMC	GEMC	GEMC	REFPROP
$T_c(K)$	305.354	302 ± 0.01	328.595	334.229	351.235	374.266	374.210
$\rho_c(g.cm^{-3})$	0.481394	0.414 ± .005	0.5059	0.5267	0.5407	0.5445	0.5119



(a)



(b)

Fig 5. Computed (a) saturated vapor and (b) liquid densities of HFO-1132a, blend¹⁻³ from MD simulation and HFC-134a from REFPROP.

Keeping the behavior of the pure refrigerants in mind, it is quite interesting to observe that the liquid density of blends¹⁻³ is increasing as the mole ratio of HFO-1132a is decreasing. However, the vapor density of blend¹ and blend² increased and for blend³, the vapor density decreased slightly compared to the vapor density of HFO-1132a. The reason behind these phenomena is the molecular weight of these pure refrigerants. HFO-1132a

is a lightweight molecule with 64.04 g/mole weight, on the other side HFC-134a is a heavy molecule because of which its tendency of entering vapor phase is less and the vapor density value is small. That is why when the percentage of HFO-1132a is higher or equal in the mixtures, the vapor density tends to be higher.

3.3 Vapor-liquid co-existence curve

Using the Equilibria module of Material studio program and by conducting GEMC simulations with 200 points, the phase diagrams of pure HFO-1132a is presented in Fig. 6. This figure also included the liquid and vapor densities that was calculated from molecular dynamics simulation shown in Fig 5. Figure 6 exhibits a good consistency of both the liquid and vapor densities in the five temperatures of 270 K, 285 K, 290 K, 293 K, 298 K, as calculated by MD simulations with the phase diagram values calculated by GEMC simulations. This consistency between the two groups of data demonstrate high reliability of the present work. The critical temperature and critical density values are also represented for pure HFO-1132a in the figure. Figure 7 displays the combined phase diagrams of pure HFO-1132a and HFC-134a and their binary mixtures. From Fig 7, it can be observed that the critical values are increasing as the mole ratio of HFO-1132a is decreasing. Moreover, it indicates that the critical points and liquid densities of blends¹⁻³ were predicted appropriately, with appropriate deviation between HFO-1132a and HFC-134a whereas the vapor density behaves depending on the proportion of HFC-134a in the blends. It is significant to point out that the saturated vapor densities for blend¹ and blend² were higher than the pure HFO-1132a and HFC-134a. This is not a common case; this is an exception. The critical temperatures and densities of HFO-1132a, blend¹⁻³ and HFC-134a were calculated using GEMC simulation and presented in Table 3. These critical values are also illustrated in Fig 7 for the refrigerants. The critical temperature and density of HFO-1132a are slightly higher than the experimental data of Perera et al [4] as found in Table 3. For pure HFC-134a the simulated data also demonstrates small deviation from the data taken from REFPROP [26].

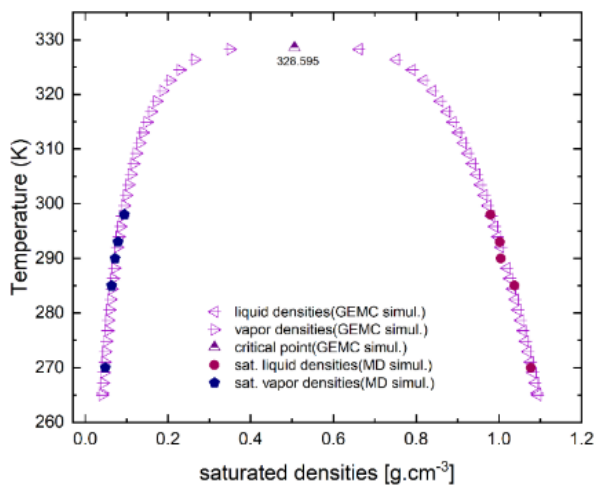


Fig. 6. Estimated phase diagram from GEMC simulation and saturated vapor liquid densities by MD simulation of pure R1132a.

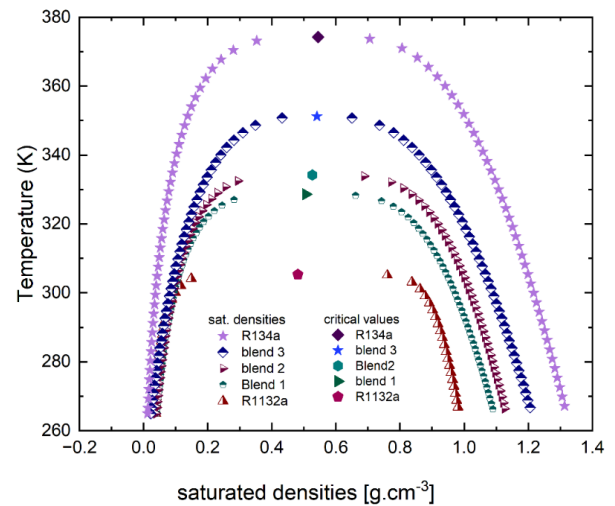
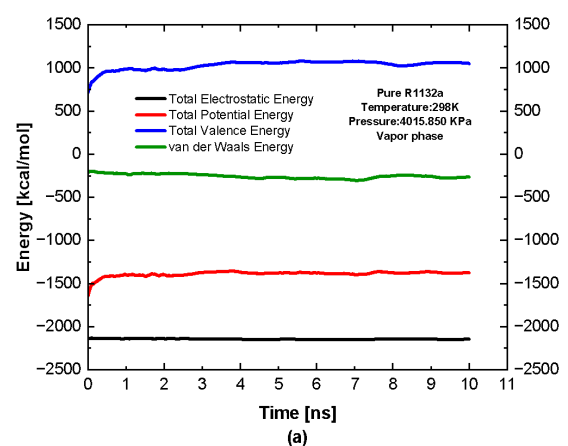


Fig 7. Estimated phase diagram from GEMC simulation of pure HFO-1132a, HFC-134a and their three blends¹⁻³.

3.4 Analysis of energy distributions

The total potential energy distribution in terms of its components electrostatic energy, total valence energy, van der Waals energy of pure HFO-1132a and its binary blends with HFC-134a are investigated at temperature 298K and corresponding pressure 4015.850 KPa to show the stability of the molecules for both vapor and liquid phases. For pure R1132a, the Fig 8 (a) shows that the total potential energy is relatively stable at around -1500 kcal/mol with van der Waals energy being the dominant components whereas the total electrostatic energy and the total valence energy remain relatively constant showing there is minor deformation of molecules. Fig 8(b) shows that the total potential energy become more negative (approximately -2000 kcal/mol) showing that the liquid phase is more stable than the vapor phase. The van der Waals energy is again the significant one and the other two energies are comparatively consistent, which validates the thermodynamic consistency of the simulation method.



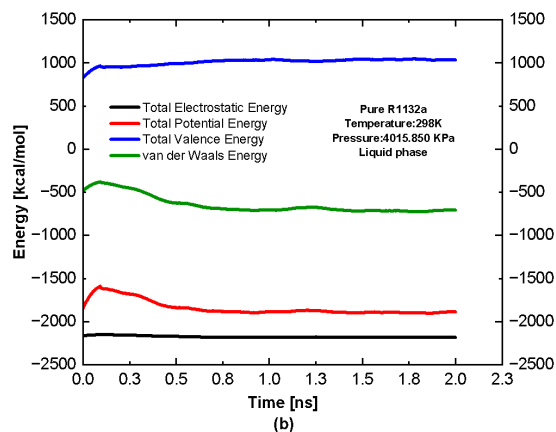


Fig 8: Total potential energy profile of pure HFO-1132a for (a) vapor Phase and (b) liquid phase at temperature 298 K.

Figure 9 shows the changes in the total potential energy of pure HFO-1132a and blends¹⁻³. It is noticed from Fig. 9 that pure R1132a has the most negative potential energy indicating that it is more stable compare the blends and blending makes the higher deformation of the molecules.

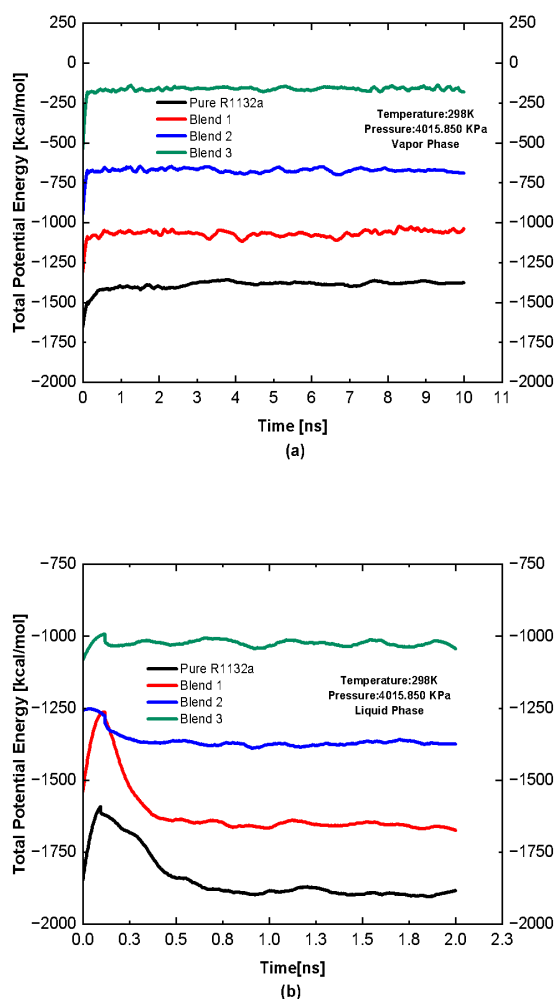


Fig 9: Comparison of total potential energy at 298K for the (a) vapor phase and (b) liquid phase of HFO-1132a and blends¹⁻³

Moreover, Fig 9(b) shows the liquid phase is more stable compare to vapor phase. In liquid phase the molecules stay closer to each other compare to vapor

phase and the intermolecular forces is stronger here which is observed in Fig 9(b), that is, the total potential energy is more negative than the vapor phase.

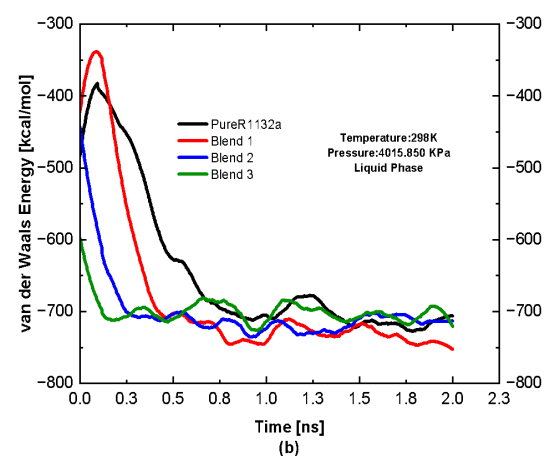
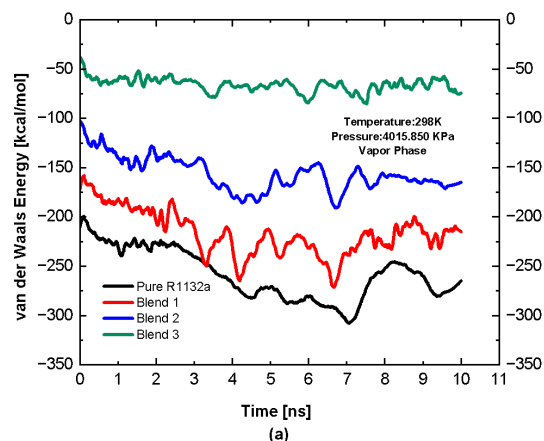


Fig 10: Comparison of van der Waals energy at 298K for the (a) vapor phase and (b) liquid phase of HFO-1132a and blends¹⁻³

Fig 10 shows the van der Waals energy of vapor and liquid phases of pure HFO-1132a and three different blends of HFO-1132a and HFC-134a. Fig 10(a) demonstrates a sequential increase of van der Waals energy as the component tending to blend³ which has 75% of HFC-134a from pure HFO-1132a. As HFC-134a has more fluorine atom and dipole that's why its van der Waals energy is higher than HFO-1132a as seen in Fig 10 (a). Fig 10 (b) displays the van der Waals energy at temperature 298 K in the liquid phase. In liquid phase, the strength of van der Waals decreases compare to vapor phase. Therefore, the value of van der Waals energy is observed higher initially and then the values dropdown and coincide with each other.

4. CONCLUSION

The saturated vapor pressures and densities of pure HFO-1132a, and its three binary blends with HFC-134a at different compositions were computed by MD simulations with a transferable COMPASS II force field. The vapor pressures of the pure compounds computed by MD simulations in the temperature range of 240 K to 300 K showed good agreement with previous experimental data, which confirmed reliable predictions for the vapor pressures of binary blends in the same temperature range. It is found that the

saturation pressures of HFO-1132a increased with temperature uniformly and consistently. Moreover, the vapor pressure dropped when HFC-134a molecule mass percentage increased and pure HFO-1132a decreased in the mixtures. Then, the saturated densities of the pure HFO-1132a and blend¹⁻³ of HFO-1132a and HFC-134a were computed with various compositions for the temperature range of 270 K to 298 K. The present GEMC simulation results for the vapor-liquid coexistence curves with critical temperatures and critical densities of the pure refrigerants as well as the blend of HFO-1132a + HFC-134a agreed well with previous experimental data and EoS available in the open literature. The total potential energy become more negative (approximately -2000 kcal/mol) in the liquid phase compare to vapor phase. The van der Waals energy is the significant one; electrostatic energy and total valence energy are comparatively consistent, which validates the thermodynamic consistency of the simulation method. The value of van der Waals energy is observed higher initially and then dropdown and coincide with each other in liquid phase for pure HFO-1132a and blend¹⁻³.

ACKNOWLEDGEMENT

The research work is performed under the Independent University VC's Research Fund 2024, Research Grant No. VCRF-SETS:24-026 of the second author in the Department of Physical Sciences. Financial contribution from the Independent University research project is acknowledged.

REFERENCE

- [1] G. J. M. Velders, D. W. Fahey, J. S. Daniel, M. McFarland, S. O. Andersen, The large contribution of projected HFC emissions to future climate forcing, *Proc. Natl Acad. Sci.* 106 (2009) 10949–10954.
- [2] R. Al-Rubaay, C. J. Seeton, R. E. Low, 1,1-difluoroethylene thermal stability, material compatibility and refrigerant/lubricant interactions study, 19th International Refrigeration and Air-Conditioning Conference at Purdue (2022).
- [3] M. A. Islam, S. Mitra, K. Thu, B. B. Saha, A Quantitative Approach to Analyze Total Equivalent Warming Impact (TEWI) for Supermarket Refrigeration System in Japan, Proceedings of 3rd International Exchange and Innovation Conference on Engineering & Sciences (IEICES), Kyushu University, Fukuoka, Japan, 2017.
- [4] U. Perera, K. Miyane, N. Sakoda, K. Thu, Y. Higashi, PvT Properties and Thermodynamic Property Correlations for the Low Global Warming Potential Hydrofluoroolefin Refrigerant R1132a (1,1 Difluoroethene), *International Journal of Thermophysics* 44 (2023) 1-30.
- [5] U. Perera, N. Sakoda, T. Miyazaki, K. Thu, Y. Higashi, Measurements of saturation pressures for the novel refrigerant R1132(E), *International Journal of Refrigeration* 135 (2022) 148-153.
- [6] A. R. Lawton, C. Rhodes, Comparison between HFCs and HFO/HFC blends in a commercial heat pump, 1st IIR international conference on the application of

HFO refrigerants, Birmingham, September 2-5(2018).

- [7] R. Low, Evaluation of potential use of R1132A as a refrigerant blend component, 1st IIR international conference on the application of HFO refrigerants, Birmingham, September 2-5 (2018).
- [8] L. Fedele, G. Lombardo, I. Greselin, D. Menegazzo, S. Bobbo, Thermophysical Properties of Low GWP Refrigerants: An Update, *International Journal of Thermophysics* 44 (2023) 1-52.
- [9] S. Tomassetti, G. D. Nicola, Saturated pressure and vapor-phase pvT measurements of 1,1-difluoroethene (R1132a), *Fluid Phase Equilibria* 533 (2021) 112939.
- [10] G. Raabe, Molecular dynamics studies on liquid-phase dynamics and structures of four different fluoropropenes and their binary mixtures with R-32 and CO₂, *The Journal of Physical Chemistry* 118 (2013) 240-254.
- [11] Y. Lee, D. Kang, D. Jung, Performance of Virtually non-flammable azeotropic HFO-1234yf/HFC-134a mixture for HFC-134a applications, *International journal of Refrigeration* 36(2013) 1203-1207.
- [12] S. Moromisato, H. Y. Tseng, G. Nagayama, Molecular Dynamics Study of Droplet Impinging/Freezing on Cold Surface, Proceedings of 10th International Exchange and Innovation Conference on Engineering & Sciences (IEICES), Kyushu University, Fukuoka, Japan, 2024.
- [13] G. Raabe, Molecular Simulation Studies on the Thermophysical Properties of the Refrigerant Blend R-445A, *Journal of Chemical & Engineering Data* 58(12) (2013) 3470-3476.
- [14] W. R. Smith, L. M. Figueroa, Y. C. Gerstenmaier, G. Raabe, Molecular Simulation for Thermodynamic Properties and Process Modeling of Refrigerants, *Journal of Chemical & Engineering Data* 59(10) (2014) 3258-3271.
- [15] M. S. Alam, J. H. Jeong, MD simulation estimation of saturation pressure and vapor-liquid equilibrium for binary blends of HFO-1234yf and HFO-1123, *Int. J. of Air-Conditioning and Refrigeration* 30(1) (2022) 1-14.
- [16] M. S. Alam, J. H. Jeong, Calculation of the thermodynamic properties of HFO/HFC-448A and HFO/HFC-449A in a saturation temperature range of 233.15 K to 343.15 K using molecular dynamics simulations, *Int. Comm. In Heat and Mass Transfer* 116 (2020) 104717.
- [17] M. S. Alam, J. H. Jeong, Thermodynamic properties and critical parameters of HFO-1123 and its binary blends with HFC-32 and HFC-134a using molecular simulations, *International Journal of Refrigeration*, 104 (2019) 311-320.
- [18] R. Hasan, S. Alam, J. H. Jeong, A molecular dynamics study of the condensation process in zeotropic R600/R290 mixtures at condensing temperatures from 240 K and 2360 K, *International Communication in Heat and Mass Transfer*, 161(2025) 108566.

- [19] H. Sun, COMPASS: an ab initio force-field optimized for condensed-phase applications overview with details on alkane and benzene compounds, *The Journal of Physical Chemistry B* 102(1998) 7338-7364.
- [20] Materials Studio 7.2, BIOVIA/Accelrys Software Inc, San Diego, California (2017).
- [21] P. H. Hünenberger, *Thermostat Algorithms for Molecular Dynamics Simulations*, *Advanced Computer Simulation Approaches for Soft Matter Sciences I*, Springer, Berlin, Heidelberg (2005) 105-149.
- [22] B. Leimkuhler, E. Noorizadeh, F. Theil, A gentle stochastic thermostat for molecular dynamics, *J. Stat. Phys.* 135 (2009) 261-277.
- [23] J. Bajars, J. Frank, B. Leimkuhler, Stochastic-dynamical thermostats for constraints and stiff restraints, *Eur. Phys. J.: Spec. Top.* 200 (2011) 131-152.
- [24] A. A. Samoletov, C. P. Dettmann, M. A. Chaplain, Thermostats for “Slow” Configurational Modes, *J. Stat. Phys.* 128 (2007) 1321-1336.
- [25] H. J. C. Berendsen, J. P. M. Postma, W. F. V. Gunsteren, A. DiNola, J. R. Haak, Molecular dynamics with coupling to an external bath, *The J. of Chem. Phys.* 81 (1984) 3684-3690.
- [26] E. W. Lemmon, M. L. Huber, M. O. McLinder, *Reference Fluid Thermodynamic and Transport Properties-REFPROP*, version 9.1, NIST standard Reference Database, U. S. A. (2013).